16th AIAA/CEAS Aeroacoustics Conference, 7-9 June 2010, Stockholm, Sweden

Sound Radiation from a Lined Exhaust Duct with Lined Afterbody

Ahmet Demir*
Department of Mathematics, Gebze Institute of Technology

and Sjoerd Rienstra†
Department of Mathematics and Computer Science, Eindhoven University of Technology

Aft fan noise radiating from a lined bypass exhaust duct with lined afterbody is modelled in a way that allows an analytical solution of generalised Wiener-Hopf type. A preliminary set of numerically evaluated examples, based on the experiments by Tester at al. seem to confirm their conclusions that the beneficial effect of a lined afterbody is mainly found without mean flow.

I. Introduction

A. The technical problem

AFT fan noise radiating from the bypass exhaust duct is usually attenuated by acoustic lining along the inside of the duct only. The unconventional treatment of the afterbody, recently proposed by Tester et al. [1–3] has been shown to provide an additional potential of damping of the order of 1 to 4 dB. This is remarkable, given the fact that most of the sound is supposed to radiate away from, rather than towards, the duct axis. In order to understand the underlying mechanisms, no-flow experiments and flow and no-flow CAA simulations have been performed, as well as comparison with a relatively simple analytical model [4] where only the afterbody is lined.

In the present paper we derive an analytical Wiener-Hopf solution of a more complete version, where both the afterbody and the main duct outer wall is lined. This should enable a comparison between a lined duct with hard walled afterbody, and a lined duct with lined afterbody (with and without mean flow). The complexity of the problem leads to quite involved analysis and laborious formulas, but eventually a numerical evaluation provides first results that seem to confirm the earlier findings of Tester et al.

B. The model problem

The typical advantages of analytic solutions (at least, potentially) like transparency and exactness have to be paid for by considerable simplifications of geometry and physical environment in combination with usually highly intricate solution methods. Nevertheless, the complementary information they provide in the form of parametric dependencies and asymptotic behaviour, compared to fully numerical and experimental approaches, can be extremely useful, while the totally uncorrelated type of errors make them ideal for verification of CAA models. Very successful in this respect are the (so-called) Munt models [5–8], based on the idealised geometry of a semi-infinite duct with wall of vanishing thickness and piece-wise uniform mean flows (originally explored by [9, 10]), solved by means of the Wiener-Hopf (WH) method. The classical configurations, with essentially only a single semi-infinite geometrical element, can be solved by means of a form of standard WH method (although the important effects of the edge singularity are not standard). As soon as more geometrical elements are involved, like a semi-infinite duct together with a semi-infinite afterbody, the solution becomes rapidly more complicated. For example, in [4] a generalisation of the WH method was used for the problems of a lined centerbody and of a lined afterbody, using the so-called "weak factorisation".

*Assistant Professor, Department of Mathematics, Gebze Institute of Technology, P.O. Box 141, Gebze, 41400 Kocaeli, Turkey
†Associate Professor, Department of Mathematics and Computer Science, Eindhoven University of Technology, P.O. Box 513, 5600 MB Eindhoven, The Netherlands, Senior Member AIAA

Very often a superficially innocent looking change of the model requires a complete re-derivation of the solution. For example, the related generalised Wiener-Hopf solution of the configuration with a centerbody that is finite is more difficult (when the inner duct exhaust plane is buried inside the outer duct [11]) or very much more difficult (when the inner exhaust plane is protruding outside the outer duct [12]). Even if the original method is generic, the details may be too different.

Also in present problem, although only a little different from [4], involves a solution procedure that is much more complicated. Again, Idemen's method [13–15] of "weak factorisation" is applied, but now the Fourier transformed boundary value problem leads to a 3×3 matrix Wiener-Hopf equation. This matrix equation system is decoupled by the introduction of an infinite sum of poles. The uncoupled scalar equations are solved independently by a standard application of analytical continuation. The final solution includes unknown coefficients which are determined by solving an infinite linear algebraic system numerically. The contribution of the instability wave is separated from the rest of the solution. The asymptotic far field is found by a standard application of the steepest descent method.

We end with some practical examples, based on the data of the experiments of [2], showing the potentials of the present model. A more extended scan through the possible parameter values is planned for the future.

To a large extent we follow the lines of [4], but at certain points the analysis differs in a non-trivial way, so we will present the derivation with details.

II. Analysis

A. Formulation of the mathematical problem

A geometry is considered which consists of a semi-infinite outer duct and a doubly infinite center body. Duct walls are assumed to be infinitely thin and they occupy the region $\{r = R_h, -\infty < z < \infty\} \cup \{r = R_d, -\infty < z < 0\}$ in circular cylindrical coordinate system (r, θ, z). The outer duct wall is rigid from outside and lined from inside while the center-body is assumed hard inside the outer duct and soft outside the outer duct. The liner impedances are denoted by Z_d (duct) and Z_h (afterbody). In the region $r > R_d$, the ambient flow is uniform and axial with density ρ_0, velocity U_0 and speed of sound c_0. In inner region $R_h < r < R_d$, there exists a jet which is also uniform and axial with density ρ_j , velocity U_j and speed of sound c_j. A vortex sheet separates these two different flow at the surface $z > 0, r = R_d$. All quantities are made dimensionless by the outer duct radius and ambient flow properties

$$r, z \sim R_d, \quad U \sim c_0, \quad \rho \sim \rho_0, \quad t \sim R_d/c_0. \tag{1}$$

The velocity potential ϕ, with $\boldsymbol{v} = \nabla\phi$, is used to obtain the acoustic pressure p, velocity $\boldsymbol{v}$ and density ρ via the

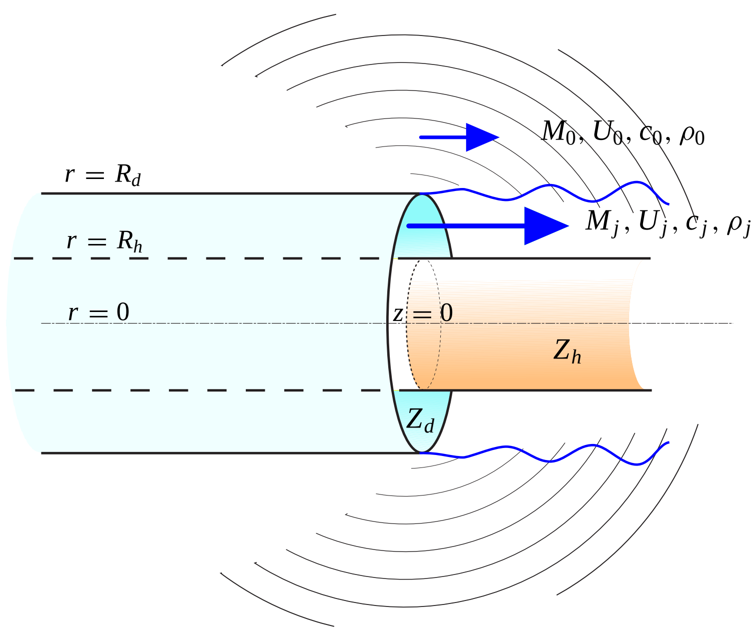

Figure 1. Geometry of the problem.

following equations [4]

$$p = -\Big(\frac{\partial\phi}{\partial t} + M_0\frac{\partial\phi}{\partial z}\Big), \qquad \boldsymbol{v} = \nabla\phi, \quad \rho = p, \qquad r > 1 \tag{2a}$$

$$p = -D_1\Big(\frac{\partial\phi}{\partial t} + M_1\frac{\partial\phi}{\partial z}\Big), \quad \boldsymbol{v} = \nabla\phi, \quad \rho = pC_1^2, \quad h < r < 1 \tag{2b}$$

$$\tag{2c}$$

where

$$M_0 = U_0/c_0, \quad M_1 = U_j/c_0, \quad C_1 = c_0/c_j, \quad D_1 = \rho_j/\rho_0, \quad h = R_h/R_d. \tag{2d}$$

From the symmetry of the geometry and the incident wave, the diffracted field will remain with the same azimuthal and time dependencies as the incident wave. It is convenient to write the total field in different regions as:

$$\phi(r,\theta,z,t) = \begin{cases} \psi_1(r,z)\,\mathrm{e}^{\mathrm{i}\omega t - \mathrm{i}m\theta}, & r > 1, \quad -\infty < z < \infty, \\ \psi_2(r,z)\,\mathrm{e}^{\mathrm{i}\omega t - \mathrm{i}m\theta} + \psi_i(r,z)\,\mathrm{e}^{\mathrm{i}\omega t - \mathrm{i}m\theta}, & h < r < 1, \quad -\infty < z < \infty, \end{cases} \tag{3}$$

where ω is the dimensionless angular frequency (Helmholtz number) and m is the circumferential order. Time dependency and the azimuthal dependency are taken proportional to $\mathrm{e}^{\mathrm{i}\omega t}$ and $\mathrm{e}^{-\mathrm{i}m\theta}$, respectively, and suppressed throughout this paper. The incident field is the mode

$$\psi_i(r,z) = A_{mn}\Psi_{mn}(r)\,\mathrm{e}^{-\mathrm{i}\omega\mu_{mn}^+ z}. \tag{4}$$

Here A_{mn} is the amplitude of the incoming wave (which will be taken unity in the analysis) and Ψ_{mn} is a linear combination of Bessel functions which satisfy the boundary conditions on the hard and soft wall:

$$\Psi_{mn}(r) = \mathcal{Y}_d(\mu_{mn}^+)J_m(\alpha_{mn}^+ r) - \mathcal{J}_d(\mu_{mn}^+)Y_m(\alpha_{mn}^+ r) \tag{5}$$

where

$$\begin{aligned} \mathcal{J}_d(u) &= \mathrm{i}D_1(1-uM_1)^2 J_m(\lambda_1\omega)/Z_d + \lambda_1 J_m'(\lambda_1\omega), \\ \mathcal{Y}_d(u) &= \mathrm{i}D_1(1-uM_1)^2 Y_m(\lambda_1\omega)/Z_d + \lambda_1 Y_m'(\lambda_1\omega). \end{aligned} \tag{6}$$

Scaled axial wavenumbers $\mu_{mn}^\pm$ are the roots of the equation

$$\mathcal{Y}_d(\mu_{mn}^\pm)J_m'(\alpha_{mn}^\pm h) - \mathcal{J}_d(\mu_{mn}^\pm)Y_m'(\alpha_{mn}^\pm h) = 0. \tag{7}$$

The signs (+) and (−) indicate right and left running modes, respectively. Axial wave numbers $\omega\mu_{mn}^\pm$ are defined as

$$\mu_{mn}^\pm = \frac{-M_1C_1^2 \pm \sqrt{C_1^2 - (1 - M_1^2C_1^2)(\alpha_{mn}^\pm/\omega)^2}}{1 - M_1^2C_1^2}, \tag{8}$$

where $\operatorname{Im}\mu_{mn}^+ \le 0$ and $\operatorname{Im}\mu_{mn}^- \ge 0$.

B. Derivation of the Wiener-Hopf System

The unknown velocity potentials $\psi_1(r,z)$ and $\psi_2(r,z)$ satisfy the convected wave equations

$$\left[\frac{\partial^2}{\partial r^2} + \frac{1}{r}\frac{\partial}{\partial r} + \frac{\partial^2}{\partial z^2} - \frac{m^2}{r^2} - \Big(\mathrm{i}\omega + M_0\frac{\partial}{\partial z}\Big)^2\right]\psi_1(r,z) = 0, \qquad r > 1, \tag{9a}$$

$$\left[\frac{\partial^2}{\partial r^2} + \frac{1}{r}\frac{\partial}{\partial r} + \frac{\partial^2}{\partial z^2} - \frac{m^2}{r^2} - C_1^2\Big(\mathrm{i}\omega + M_1\frac{\partial}{\partial z}\Big)^2\right]\psi_2(r,z) = 0, \quad h < r < 1. \tag{9b}$$

A solution to these equations can be found via Fourier transformation along z, such that

$$\psi_1(r,z) = \frac{\omega}{2\pi}\int_L A(u)H_m^{(2)}(\lambda_0\omega r)\,\mathrm{e}^{-\mathrm{i}\omega uz}\,\mathrm{d}u \tag{10a}$$

$$\psi_2(r,z) = \frac{\omega}{2\pi}\int_L \big[B(u)J_m(\lambda_1\omega r) + C(u)Y_m(\lambda_1\omega r)\big]\,\mathrm{e}^{-\mathrm{i}\omega uz}\,\mathrm{d}u, \tag{10b}$$

where L is a suitable inverse Fourier transform integration contour along or near the real axis in the complex u-domain (see [4]). J_m and Y_m are the Bessel and Neumann functions of order m, $H_m^{(2)} = J_m - \mathrm{i}Y_m$ is the Hankel function of the second type. λ_0 and λ_1 are square root functions which are defined as

$$\begin{aligned} \lambda_0(u) &= \sqrt{(1-uM_0)^2 - u^2}, \qquad \mathrm{Im}(\lambda_0) \le 0, \\ \lambda_1(u) &= \sqrt{C_1^2(1-uM_1)^2 - u^2}, \quad \mathrm{Im}(\lambda_1) \le 0. \end{aligned} \tag{11}$$

Branch cuts for λ_0 are taken on the line from $1/(1+M_0)$ to $+\infty$ and from $-\infty$ to $-1/(1-M_0)$. Similarly for λ_1 branch cuts start from $C_1/(1+M_1C_1)$ to $+\infty$ and from $-\infty$ to $-C_1/(1-M_1C_1)$.

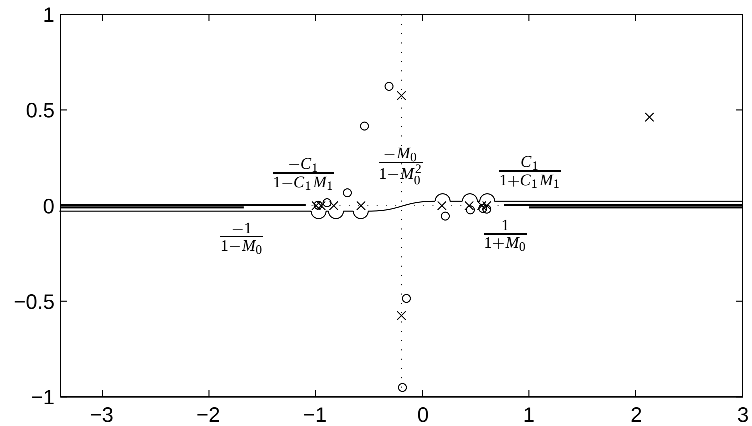

Figure 2. Sketch of complex u-plane with Fourier contour, branch cuts and axial modal wavenumbers.

As usual in this kind of Wiener-Hopf problems, the analysis will be facilitated by giving frequency ω a small negative imaginary part, written as $\omega = |\omega|\,\mathrm{e}^{-\mathrm{i}\delta}$. This will lead to an infinite strip S in the complex u-plane through the origin, inclined under an angle δ, and just small enough to fit between the branch cuts of λ_0 and λ_1, along which the Wiener-Hopf equation will be formulated. Eventually $\delta \to 0$ and strip S will merge into the real axis.

Equations for the unknown spectral coefficients $A(u)$, $B(u)$ and $C(u)$ will be obtained below from boundary conditions and relations of continuity.

The outer side of the outer duct wall is rigid, so that

$$\frac{\partial}{\partial r}\psi_1(1,z) = 0, \qquad z < 0 \tag{12a}$$

The Ingard-Myers boundary condition [16, 17] along the lined inside part of the outer duct wall can be written as

$$\left(\frac{\partial}{\partial r} + \frac{D_1}{\mathrm{i}\omega Z_d}\Big(\mathrm{i}\omega + M_1\frac{\partial}{\partial z}\Big)^2\right)\psi_2(1,z) = 0, \qquad -\infty < z < 0. \tag{12b}$$

The same condition along the lined afterbody can be written as

$$\left(\frac{\partial}{\partial r} - \frac{D_1}{\mathrm{i}\omega Z_h}\Big(\mathrm{i}\omega + M_1\frac{\partial}{\partial z}\Big)^2\right)\big[\psi_2(h,z) + \psi_i(h,z)\big] = 0, \qquad 0 < z < \infty \tag{12c}$$

The inner duct wall inside the duct is rigid, so that

$$\frac{\partial}{\partial r}\psi_2(h,z) = 0, \qquad z < 0 \tag{12d}$$

The pressure is continuous across the vortex sheet along $r = 1$, downstream the trailing edge at $z = 0$, so

$$D_1\left(\mathrm{i}\omega + M_1\frac{\partial}{\partial z}\right)[\psi_2(1,z) + \psi_i(1,z)] = \left(\mathrm{i}\omega + M_0\frac{\partial}{\partial z}\right)\psi_1(1,z), \qquad z > 0. \tag{12e}$$

By defining the complex radial displacement of the vortex sheet by $r = 1 + \xi(z)\,\mathrm{e}^{\mathrm{i}\omega t - \mathrm{i}m\theta}$, we obtain

$$\Big(\mathrm{i}\omega + M_0 \frac{\partial}{\partial z}\Big)\,\xi(z) = \frac{\partial}{\partial r}\psi_1(1, z), \qquad z > 0, \tag{12f}$$

$$\Big(\mathrm{i}\omega + M_1 \frac{\partial}{\partial z}\Big)\,\xi(z) = \frac{\partial}{\partial r}\big[\psi_2(1, z) + \psi_i(1, z)\big], \qquad z > 0. \tag{12g}$$

which implies the condition of continuity of particle displacement.

In addition to these boundary conditions and continuity relations, we assume that the field radiates outward to infinity and does not reflect backward. A generalized Kutta condition, defining via a parameter Γ the amount of vorticity shed from the cylinder trailing edge, is also imposed at the edge of the cylinder. The full Kutta condition $\Gamma = 1$ implies that the pressure is finite at the edge, and the velocity potential is finite and behaves, similar to the vortex sheet displacement, like

$$\xi(z), \phi(1, z) = \mathcal{O}(z^{3/2}) \qquad z \downarrow 0 \tag{13}$$

We introduce the half-plane analytical functions $\Phi_1^{\pm}$, $F_{\pm}$, $G^{\pm}$

$$\Phi_+(u) = \int_0^\infty \frac{\partial}{\partial r}\psi_2(h, z)\,\mathrm{e}^{\mathrm{i}\omega u z}\,\mathrm{d}z, \tag{14a}$$

$$\Phi_-(u) = \int_{-\infty}^0 \Big[\frac{\partial}{\partial r}\psi_2(h, z) - \frac{D_1}{\mathrm{i}\omega Z_h}\Big(\mathrm{i}\omega + M_1 \frac{\partial}{\partial z}\Big)^2 \psi_2(h, z)\Big]\,\mathrm{e}^{\mathrm{i}\omega u z}\,\mathrm{d}z, \tag{14b}$$

$$F_+(u) = \int_0^\infty \xi(z)\,\mathrm{e}^{\mathrm{i}\omega u z}\,\mathrm{d}z, \tag{14c}$$

$$F_-(u) = \int_{-\infty}^0 \frac{\partial}{\partial r}\psi_2(1, z)\,\mathrm{e}^{\mathrm{i}\omega u z}\,\mathrm{d}z, \tag{14d}$$

$$G_+(u) = \int_0^\infty \Big[\frac{\partial}{\partial r}\psi_2(1, z) + \frac{D_1}{\mathrm{i}\omega Z_d}\Big(\mathrm{i}\omega + M_1 \frac{\partial}{\partial z}\Big)^2 \psi_2(1, z)\Big]\,\mathrm{e}^{\mathrm{i}\omega u z}\,\mathrm{d}z. \tag{14e}$$

$$G_-(u) = \int_{-\infty}^0 \Big[\Big(\mathrm{i}\omega + M_0 \frac{\partial}{\partial z}\Big)\psi_1(1, z) - D_1\Big(\mathrm{i}\omega + M_1 \frac{\partial}{\partial z}\Big)\psi_2(1, z)\Big]\,\mathrm{e}^{\mathrm{i}\omega u z}\,\mathrm{d}z \tag{14f}$$

During the course of analysis we will use the fact that the behaviour of a function $H^+(u) = \int_0^\infty h(z)\,\mathrm{e}^{\mathrm{i}\omega u z}\,\mathrm{d}z$ for $|u| \to \infty$ is related to the (anticipated) behaviour of $h(z)$ for $z \downarrow 0$ in the following way [18]. If $h(z) = O(z^\eta)$, then $H^+(u) = O(u^{-\eta-1})$.

Application of the boundary conditions on $r = h$ and $r = 1$ gives

$$\lambda_1\omega\big(B(u)J_m'(\lambda_1\omega h) + C(u)Y_m'(\lambda_1\omega h)\big) = \Phi_+(u) \tag{15a}$$

$$\omega\big(B(u)\mathcal{J}_h(u) + C(u)\mathcal{Y}_h(u)\big) = \Phi_-(u) - D_1\Psi_{mn}(h)\frac{(1 - M_1\mu_{mn}^+)^2}{Z_h(u - \mu_{mn}^+)}, \tag{15b}$$

$$\lambda_0 A(u) H_m^{(2)\prime}(\lambda_0\omega) = \mathrm{i}(1 - uM_0)F_+(u), \tag{15c}$$

$$\lambda_1\omega\big(B(u)J_m'(\lambda_1\omega) + C(u)Y_m'(\lambda_1\omega)\big) = \mathrm{i}\omega(1 - uM_1)F_+(u) + F_-(u) + \frac{\Psi_{mn}'(1)}{\mathrm{i}\omega(u - \mu_{mn}^+)} \tag{15d}$$

$$\omega\big(B(u)\mathcal{J}_d(u) + C(u)\mathcal{Y}_d(u)\big) = G_+(u), \tag{15e}$$

$$\begin{aligned}&\mathrm{i}\omega(1 - uM_0)A(u)H_m^{(2)}(\lambda_0\omega)\ldots\\ &\quad -\mathrm{i}\omega D_1(1 - uM_1)\big(B(u)J_m(\lambda_1\omega) + C(u)Y_m(\lambda_1\omega)\big) = G_-(u) - D_1\Psi_{mn}(1)\frac{1 - \mu_{mn}^+ M_1}{u - \mu_{mn}^+}.\end{aligned} \tag{15f}$$

where

$$\begin{aligned}\mathcal{J}_h(u) &= -\mathrm{i}D_1(1 - uM_1)^2 J_m(\lambda_1\omega h)/Z_h + \lambda_1 J_m'(\lambda_1\omega h),\\ \mathcal{Y}_h(u) &= -\mathrm{i}D_1(1 - uM_1)^2 Y_m(\lambda_1\omega h)/Z_h + \lambda_1 Y_m'(\lambda_1\omega h).\end{aligned} \tag{16}$$

$A(u)$, $B(u)$ and $C(u)$ may be eliminated as follows

$$A(u) = \mathrm{i}\frac{1 - uM_0}{\lambda_0 H_m^{(2)\prime}(\lambda_0\omega)}F_+(u), \tag{17a}$$

$$B(u) = \frac{\mathcal{Y}_d(u)\Phi_+(u) - \lambda_1 Y_m'(\lambda_1\omega h)G_+(u)}{\lambda_1\omega\big(\mathcal{Y}_d(u)J_m'(\lambda_1\omega h) - \mathcal{J}_d(u)Y_m'(\lambda_1\omega h)\big)}, \tag{17b}$$

$$C(u) = -\frac{\mathcal{J}_d(u)\Phi_+(u) - \lambda_1 J_m'(\lambda_1\omega h)G_+(u)}{\lambda_1\omega\big(\mathcal{Y}_d(u)J_m'(\lambda_1\omega h) - \mathcal{J}_d(u)Y_m'(\lambda_1\omega h)\big)}, \tag{17c}$$

leading to

$$\frac{1}{\lambda_1}\frac{\mathcal{J}_d(u)\mathcal{Y}_h(u) - \mathcal{Y}_d(u)\mathcal{J}_h(u)}{\mathcal{J}_d(u)Y_m'(\lambda_1\omega h) - \mathcal{Y}_d(u)J_m'(\lambda_1\omega h)}\Phi_+(u) + \frac{\mathcal{J}_h(u)Y_m'(\lambda_1\omega h) - \mathcal{Y}_h(u)J_m'(\lambda_1\omega h)}{\mathcal{J}_d(u)Y_m'(\lambda_1\omega h) - \mathcal{Y}_d(u)J_m'(\lambda_1\omega h)}G_+ = \Phi_-(u) - D_1\Psi_{mn}(h)\frac{(1-\mu_{mn}^+M_1)^2}{Z_h(u-\mu_{mn}^+)}, \tag{18a}$$

$$\frac{\mathcal{J}_d(u)Y_m'(\lambda_1\omega) - \mathcal{Y}_d(u)J_m'(\lambda_1\omega)}{\mathcal{J}_d(u)Y_m'(\lambda_1\omega h) - \mathcal{Y}_d(u)J_m'(\lambda_1\omega h)}\Phi_+(u) + \lambda_1\frac{J_m'(\lambda_1\omega)Y_m'(\lambda_1\omega h) - Y_m'(\lambda_1\omega)J_m'(\lambda_1\omega h)}{\mathcal{J}_d(u)Y_m'(\lambda_1\omega h) - \mathcal{Y}_d(u)J_m'(\lambda_1\omega h)}G_+(u) = \mathrm{i}\omega(1-uM_1)F_+(u) + F_-(u) + \frac{\Psi_{mn}'(1)}{\mathrm{i}\omega(u-\mu_{mn}^+)}, \tag{18b}$$

$$-\mathrm{i}D_1(1-uM_1)\left[\frac{1}{\lambda_1}\frac{\mathcal{J}_d(u)Y_m(\lambda_1\omega) - \mathcal{Y}_d(u)J_m(\lambda_1\omega)}{\mathcal{J}_d(u)Y_m'(\lambda_1\omega h) - \mathcal{Y}_d(u)J_m'(\lambda_1\omega h)}\Phi_+(u) + \frac{J_m(\lambda_1\omega)Y_m'(\lambda_1\omega h) - Y_m(\lambda_1\omega)J_m'(\lambda_1\omega h)}{\mathcal{J}_d(u)Y_m'(\lambda_1\omega h) - \mathcal{Y}_d(u)J_m'(\lambda_1\omega h)}G_+(u)\right] - \omega(1-uM_0)^2\frac{H_m^{(2)}(\lambda_0\omega)}{\lambda_0 H_m^{(2)\prime}(\lambda_0\omega)}F_+(u) = G_-(u) - D_1\Psi_{mn}(1)\frac{1-\mu_{mn}^+M_1}{u-\mu_{mn}^+}. \tag{18c}$$

We define the kernels $N(u)$, $L(u)$, $K(u)$ by

$$N(u) = \lambda_1\frac{\mathcal{J}_d(u)Y_m'(\lambda_1\omega h) - \mathcal{Y}_d(u)J_m'(\lambda_1\omega h)}{\mathcal{J}_d(u)\mathcal{Y}_h(u) - \mathcal{Y}_d(u)\mathcal{J}_h(u)}, \tag{19a}$$

$$L(u) = \lambda_1\frac{J_m'(\lambda_1\omega)\mathcal{Y}_h(u) - Y_m'(\lambda_1\omega)\mathcal{J}_h(u)}{\mathcal{J}_d(u)\mathcal{Y}_h(u) - \mathcal{Y}_d(u)\mathcal{J}_h(u)}, \tag{19b}$$

$$K(u) = D_1(1-uM_1)^2\frac{J_m(\lambda_1\omega)\mathcal{Y}_h(u) - Y_m(\lambda_1\omega)\mathcal{J}_h(u)}{\lambda_1\big(J_m'(\lambda_1\omega)\mathcal{Y}_h(u) - Y_m'(\lambda_1\omega)\mathcal{J}_h(u)\big)} - (1-uM_0)^2\frac{H_m^{(2)}(\lambda_0\omega)}{\lambda_0 H_m^{(2)\prime}(\lambda_0\omega)}, \tag{19c}$$

and note the following Wronskian-type relations

$$\begin{aligned}
\mathcal{J}_d(u)Y_m(\lambda_1\omega) - \mathcal{Y}_d(u)J_m(\lambda_1\omega) &= -\frac{2}{\pi\omega}, \\
\mathcal{J}_d(u)Y_m'(\lambda_1\omega) - \mathcal{Y}_d(u)J_m'(\lambda_1\omega) &= \frac{2\mathrm{i}D_1(1-uM_1)^2}{Z_d\pi\lambda_1\omega}, \\
\mathcal{J}_h(u)Y_m(\lambda_1\omega h) - \mathcal{Y}_h(u)J_m(\lambda_1\omega h) &= -\frac{2}{\pi\omega h}, \\
\mathcal{J}_h(u)Y_m'(\lambda_1\omega h) - \mathcal{Y}_h(u)J_m'(\lambda_1\omega h) &= -\frac{2\mathrm{i}D_1(1-uM_1)^2}{Z_h\pi\lambda_1\omega h}.
\end{aligned} \tag{20}$$

Then equation (18a) can be recast into

$$\Phi_+(u) - N(u)\left\{\Phi_-(u) - D_1\Psi_{mn}(h)\frac{(1-\mu_{mn}^+M_1)^2}{Z_h(u-\mu_{mn}^+)}\right\} = \frac{2\mathrm{i}D_1(1-uM_1)^2}{\pi\omega h Z_h\big[\mathcal{J}_d(u)\mathcal{Y}_h(u) - \mathcal{Y}_d(u)\mathcal{J}_h(u)\big]}G_+(u), \tag{21a}$$

Φ_+ can be eliminated from equation (18b), leading to

$$L(u)G_+(u) - \mathrm{i}\omega(1-uM_1)F_+(u) = F_-(u) + \frac{\Psi_{mn}'(1)}{\mathrm{i}\omega(u-\mu_{mn}^+)} - \frac{2\mathrm{i}D_1(1-uM_1)^2}{\pi\omega Z_d\big[\mathcal{J}_d(u)\mathcal{Y}_h(u) - \mathcal{Y}_d(u)\mathcal{J}_h(u)\big]}\left\{\Phi_-(u) - D_1\Psi_{mn}(h)\frac{(1-\mu_{mn}^+M_1)^2}{Z_h(u-\mu_{mn}^+)}\right\}, \tag{21b}$$

By eliminating Φ_+ and G_+ we find finally from equation (18c)

$$\omega K(u)F_+(u) + \frac{2\mathrm{i}D_1(1-uM_1)}{\pi\lambda_1\omega\big[J_m'(\lambda_1\omega)\mathcal{Y}_h(u) - Y_m'(\lambda_1\omega)\mathcal{J}_h(u)\big]}\left\{\Phi_-(u) - D_1\Psi_{mn}(h)\frac{(1-\mu_{mn}^+M_1)^2}{Z_h(u-\mu_{mn}^+)}\right\} = G_-(u)+$$
$$\mathrm{i}D_1(1-uM_1)\frac{\big[J_m(\lambda_1\omega)\mathcal{Y}_h(u) - Y_m(\lambda_1\omega)\mathcal{J}_h(u)\big]}{\lambda_1\big[J_m'(\lambda_1\omega)\mathcal{Y}_h(u) - Y_m'(\lambda_1\omega)\mathcal{J}_h(u)\big]}\left\{F_-(u) + \frac{\Psi_{mn}'(1)}{\mathrm{i}\omega(u-\mu_{mn}^+)}\right\} - D_1\Psi_{mn}(1)\frac{1-\mu_{mn}^+M_1}{u-\mu_{mn}^+}. \quad (21c)$$

These are the three coupled Wiener-Hopf equations to be solved.

Note

We note in passing that we can eliminate G_+ from equations (21a) and (21b) to obtain

$$\Phi_+(u) - \widetilde{N}(u)\left\{\Phi_-(u) - D_1\Psi_{mn}(h)\frac{(1-\mu_{mn}^+M_1)^2}{Z_h(u-\mu_{mn}^+)}\right\} =$$
$$\frac{2\mathrm{i}D_1(1-uM_1)^2}{\pi\lambda_1\omega h Z_h\big[J_m'(\lambda_1\omega)\mathcal{Y}_h(u) - Y_m'(\lambda_1\omega)\mathcal{J}_h(u)\big]}\left(\mathrm{i}\omega(1-uM_1)F_+(u) + F_-(u) + \frac{\Psi_{mn}'(1)}{\mathrm{i}\omega(u-\mu_{mn}^+)}\right),$$

with

$$\widetilde{N}(u) = \lambda_1\frac{J_m'(\lambda_1\omega)Y_m'(\lambda_1\omega h) - Y_m'(\lambda_1\omega)J_m'(\lambda_1\omega h)}{J_m'(\lambda_1\omega)\mathcal{Y}_h(u) - Y_m'(\lambda_1\omega)\mathcal{J}_h(u)}$$

For a hard-walled duct, $F_-(u)$ and $\Psi_{mn}'(1)$ vanish, and the expression is equivalent to (28a) and (28b) of [4]. In the present problem on the other hand, the presence of F_- apparently prohibits finding a split of the equations in the way done in [4], and we have to retain the set of 3 equations.

C. Factorisation of the kernels

The crucial step in the Wiener-Hopf method is to split the kernel functions N, L and K as a ratio of two functions analytic in the upper and lower half complex u-plane,

$$N(u) = \frac{N_+(u)}{N_-(u)}, \quad L(u) = \frac{L_+(u)}{L_-(u)}, \quad K(u) = \frac{K_+(u)}{K_-(u)}. \quad (22)$$

For the meromorphic functions N and L this is relatively easy. For K some care is required because of a physical argument with respect to an instability pole $u = u_0$.

By taking a closed contour withing the strip (see [5,19]) and using Cauchy's theorem, $N_\pm$ and $L_\pm$ can be evaluated in the classical way by the following integrals [18]

$$\log N_\pm(\xi) = \frac{1}{2\pi\mathrm{i}}\int_{C_\pm}\frac{\log[N(u)]}{u-\xi}\,\mathrm{d}u, \qquad \log L_\pm(\xi) = \frac{1}{2\pi\mathrm{i}}\int_{C_\pm}\frac{\log[L(u)]}{u-\xi}\,\mathrm{d}u. \quad (23)$$

When δ is taken to zero, the contours $C_\pm$ coincide with the real axis at the respective sides of the branch cuts of λ_0 and λ_1.

The behaviour for $|u| \to \infty$ is given by

$$N_+(u), L_+(u) \sim u^{-1/2}, \qquad N_-(u), L_-(u) \sim u^{1/2}.$$

In the same way as presented in [19], the zero $u = u_0$ of $K(u)$, found in the complex upper half plane, but being associated to the right-running Helmholtz instability of the vortex sheet really belonging to the the lower half plane, is brought to the "other side" by producing regular split functions $\hat{K}_+$ and $\hat{K}_-$ and then keeping

$$K_+(u) = \hat{K}_+(u)(u-u_0), \quad K_-(u) = \hat{K}_-(u)(u-u_0)$$

together. Since $\hat{K}_+(u) \sim u^{1/2}$ and $\hat{K}_-(u) \sim u^{-1/2}$, we have

$$K_+(u) \sim u^{3/2}, \qquad K_-(u) \sim u^{1/2}.$$

The role of u_0 is very important for the application of the Kutta condition (see [4]).

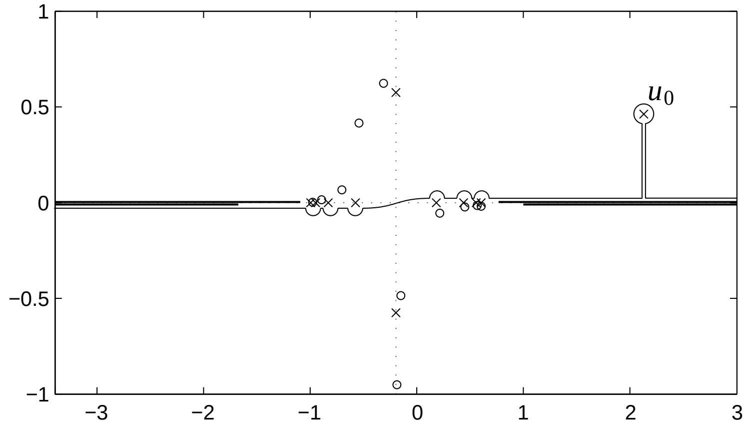

Figure 3. Sketch of deformed integration contour to include instability pole u_0.

D. Wiener-Hopf Solution by Weak Factorisation

Multiplying equation (21a) by $1/N_+(u)$ and subtracting from both sides the pole in $u = \mu^+_{mn}$ yields

$$\frac{\Phi_+(u)}{N_+(u)} - \frac{2\mathrm{i}D_1(1-uM_1)^2}{\pi\omega h Z_h\big[\mathcal{J}_d(u)\mathcal{Y}_h(u) - \mathcal{Y}_d(u)\mathcal{J}_h(u)\big]}\frac{G_+(u)}{N_+(u)} + \frac{D_1\Psi_{mn}(h)(1-\mu^+_{mn}M_1)^2}{Z_h N_-(\mu^+_{mn})(u-\mu^+_{mn})} = \\ \frac{1}{N_-(u)}\left\{\Phi_-(u) - D_1\Psi_{mn}(h)\frac{(1-\mu^+_{mn}M_1)^2}{Z_h(u-\mu^+_{mn})}\right\} + \frac{D_1\Psi_{mn}(h)(1-\mu^+_{mn}M_1)^2}{Z_h N_-(\mu^+_{mn})(u-\mu^+_{mn})} \quad (24a)$$

Multiplying equation (21b) by $L_-(u)$ and noting that the poles in $u = \mu^+_{mn}$ cancel out, we obtain

$$L_+(u)G_+(u) - \mathrm{i}\omega(1-uM_1)F_+(u)\frac{L_+(u)}{\lambda_1}\frac{\mathcal{J}_d(u)\mathcal{Y}_h(u) - \mathcal{Y}_d(u)\mathcal{J}_h(u)}{J'_m(\lambda_1\omega)\mathcal{Y}_h(u) - Y'_m(\lambda_1\omega)\mathcal{J}_h(u)} = F_-(u)L_-(u) + \\ \frac{\Psi'_{mn}(1)}{\mathrm{i}\omega(u-\mu^+_{mn})}L_-(u) - \frac{2\mathrm{i}D_1(1-uM_1)^2}{\pi\omega Z_d\big[\mathcal{J}_d(u)\mathcal{Y}_h(u) - \mathcal{Y}_d(u)\mathcal{J}_h(u)\big]}\left\{\Phi_-(u) - D_1\Psi_{mn}(h)\frac{(1-\mu^+_{mn}M_1)^2}{Z_h(u-\mu^+_{mn})}\right\}L_-(u). \quad (24b)$$

Multiplying equation (21c) by $K_-(u)$ and again noting that the poles in $u = \mu^+_{mn}$ cancel out, we get

$$\omega K_+(u)F_+(u) = G_-(u)K_-(u) - D_1\Psi_{mn}(1)\frac{1-\mu^+_{mn}M_1}{u-\mu^+_{mn}}K_-(u) \\ - \frac{2\mathrm{i}D_1(1-uM_1)}{\pi\lambda_1\omega\big[J'_m(\lambda_1\omega)\mathcal{Y}_h(u) - Y'_m(\lambda_1\omega)\mathcal{J}_h(u)\big]}\left\{\Phi_-(u) - D_1\Psi_{mn}(h)\frac{(1-\mu^+_{mn}M_1)^2}{Z_h(u-\mu^+_{mn})}\right\}K_-(u) \\ + \mathrm{i}D_1(1-uM_1)\frac{J_m(\lambda_1\omega)\mathcal{Y}_h(u) - Y_m(\lambda_1\omega)\mathcal{J}_h(u)}{\lambda_1\big[J'_m(\lambda_1\omega)\mathcal{Y}_h(u) - Y'_m(\lambda_1\omega)\mathcal{J}_h(u)\big]}\left\{F_-(u) + \frac{\Psi'_{mn}(1)}{\mathrm{i}\omega(u-\mu^+_{mn})}\right\}K_-(u). \quad (24c)$$

Our goal is that the Wiener-Hopf equations (21a,21b,21c) are rewritten in such a way that we have on the left hand side a function that is analytic in the upper half u-plane, and on the right hand side analytic in the lower half u-plane, while both half planes have a strip in common as long as $\delta > 0$. This is almost but not yet achieved by the equations (24a,24b,24c).

Take for example equation (24a). The right-hand side is analytic on the lower half-plane but the analyticity of the left hand side is violated by the zeros $u = \sigma^-_{mp}$ of the denominator at the upper half-plane, given by

$$\mathcal{J}_d(\sigma^-_{mp})\mathcal{Y}_h(\sigma^-_{mp}) - \mathcal{Y}_d(\sigma^-_{mp})\mathcal{J}_h(\sigma^-_{mp}) = 0.$$

The method of Weak Factorization involves subtracting the residue contributions from these poles, such that the left hand side becomes analytic in the upper half plane, as follows

$$\frac{\Phi_+(u)}{N_+(u)} - \frac{2\mathrm{i}D_1(1-uM_1)^2}{\pi\omega h Z_h\big[\mathcal{J}_d(u)\mathcal{Y}_h(u)-\mathcal{Y}_d(u)\mathcal{J}_h(u)\big]}\frac{G_+(u)}{N_+(u)} + \frac{D_1\Psi_{mn}(h)(1-\mu_{mn}^+M_1)^2}{Z_hN_-(\mu_{mn}^+)(u-\mu_{mn}^+)} - \sum_{p=1}^{\infty}\frac{a_{mp}^+}{u-\sigma_{mp}^-} =$$

$$\frac{1}{N_-(u)}\left\{\Phi_-(u) - D_1\Psi_{mn}(h)\frac{(1-\mu_{mn}^+M_1)^2}{Z_h(u-\mu_{mn}^+)}\right\} + \frac{D_1\Psi_{mn}(h)(1-\mu_{mn}^+M_1)^2}{Z_hN_-(\mu_{mn}^+)(u-\mu_{mn}^+)} - \sum_{p=1}^{\infty}\frac{a_{mp}^+}{u-\sigma_{mp}^-} \tag{25a}$$

where

$$a_{mp}^+ = \frac{-2\mathrm{i}D_1(1-\sigma_{mp}^-M_1)^2}{\pi\omega h Z_h\frac{\mathrm{d}}{\mathrm{d}u}\big[\mathcal{J}_d(u)\mathcal{Y}_h(u)-\mathcal{Y}_d(u)\mathcal{J}_h(u)\big]_{u=\sigma_{mp}^-}}\frac{G_+(\sigma_{mp}^-)}{N_+(\sigma_{mp}^-)}. \tag{25b}$$

From Liouville's theorem it follows that the left and right hand sides define the same analytic function. Anticipating smooth enough behaviour at $z=0$ this function is zero, leading to

$$\frac{\Phi_+(u)}{N_+(u)} - \frac{2\mathrm{i}D_1(1-uM_1)^2}{\pi\omega h Z_h\big[\mathcal{J}_d(u)\mathcal{Y}_h(u)-\mathcal{Y}_d(u)\mathcal{J}_h(u)\big]}\frac{G_+(u)}{N_+(u)} = \sum_{p=1}^{\infty}\frac{a_{mp}^+}{u-\sigma_{mp}^-} - \frac{D_1\Psi_{mn}(h)(1-\mu_{mn}^+M_1)^2}{Z_hN_-(\mu_{mn}^+)(u-\mu_{mn}^+)}, \tag{25c}$$

$$\frac{1}{N_-(u)}\left\{\Phi_-(u) - D_1\Psi_{mn}(h)\frac{(1-\mu_{mn}^+M_1)^2}{Z_h(u-\mu_{mn}^+)}\right\} = \sum_{p=1}^{\infty}\frac{a_{mp}^+}{u-\sigma_{mp}^-} - \frac{D_1\Psi_{mn}(h)(1-\mu_{mn}^+M_1)^2}{Z_hN_-(\mu_{mn}^+)(u-\mu_{mn}^+)}. \tag{25d}$$

Next we consider equation (24b). Here, the analyticity is violated by the zeros $u=\sigma_{mp}^+$ in the upper, and $u=\kappa_{mp}^-$ in the lower half plane, given by

$$\begin{aligned}&\mathcal{J}_d(\sigma_{mp}^+)\mathcal{Y}_h(\sigma_{mp}^+) - \mathcal{Y}_d(\sigma_{mp}^+)\mathcal{J}_h(\sigma_{mp}^+) = 0,\\ &J_m'(\beta_{mp}^-)\mathcal{Y}_h(\kappa_{mp}^-) - Y_m'(\beta_{mp}^-)\mathcal{J}_h(\kappa_{mp}^-) = 0,\ \text{where } \beta_{mp}^- = \lambda_1(\kappa_{mp}^-)\omega.\end{aligned}$$

(Note that $\lambda_1=0$ is not among the poles.) By subtracting the respective poles on both sides, we obtain again expressions, regular in upper and lower plane:

$$\begin{aligned}&L_+(u)G_+(u) - \mathrm{i}\omega(1-uM_1)F_+(u)\frac{L_+(u)}{\lambda_1}\frac{\mathcal{J}_d(u)\mathcal{Y}_h(u)-\mathcal{Y}_d(u)\mathcal{J}_h(u)}{J_m'(\lambda_1\omega)\mathcal{Y}_h(u)-Y_m'(\lambda_1\omega)\mathcal{J}_h(u)} - \sum_{p=1}^{\infty}\frac{c_{mp}^+}{u-\kappa_{mp}^-} - \sum_{p=1}^{\infty}\frac{a_{mp}^-}{u-\sigma_{mp}^+} =\\ &\quad -\frac{2\mathrm{i}D_1(1-uM_1)^2L_-(u)}{\pi\omega Z_d\big[\mathcal{J}_d(u)\mathcal{Y}_h(u)-\mathcal{Y}_d(u)\mathcal{J}_h(u)\big]}\left\{\Phi_-(u) - D_1\Psi_{mn}(h)\frac{(1-\mu_{mn}^+M_1)^2}{Z_h(u-\mu_{mn}^+)}\right\}\\ &\quad - \sum_{p=1}^{\infty}\frac{c_{mp}^+}{u-\kappa_{mp}^-} - \sum_{p=1}^{\infty}\frac{a_{mp}^-}{u-\sigma_{mp}^+} + L_-(u)\left\{F_-(u) + \frac{\Psi_{mn}'(1)}{\mathrm{i}\omega(u-\mu_{mn}^+)}\right\},\end{aligned} \tag{26a}$$

where

$$c_{mp}^+ = \frac{2\omega D_1(1-\kappa_{mp}^-M_1)^3F_+(\kappa_{mp}^-)L_+(\kappa_{mp}^-)\mathcal{J}_h(\kappa_{mp}^-)}{\pi Z_d\beta_{mp}^-J_m'(\beta_{mn}^-)\frac{\mathrm{d}}{\mathrm{d}u}[J_m'(\lambda_1\omega)\mathcal{Y}_h(u) - Y_m'(\lambda_1\omega)\mathcal{J}_h(u)]_{u=\kappa_{mp}^-}}, \tag{26b}$$

$$a_{mp}^- = -\frac{2\mathrm{i}D_1(1-\sigma_{mp}^+M_1)^2L_-(\sigma_{mp}^+)}{\pi\omega Z_d\frac{\mathrm{d}}{\mathrm{d}u}\big[\mathcal{J}_d(u)\mathcal{Y}_h(u)-\mathcal{Y}_d(u)\mathcal{J}_h(u)\big]_{u=\sigma_{mp}^+}}\left\{\Phi_-(\sigma_{mp}^+) - D_1\Psi_{mn}(h)\frac{(1-\mu_{mn}^+M_1)^2}{Z_h(\sigma_{mp}^+-\mu_{mn}^+)}\right\}. \tag{26c}$$

and use is made of the relation

$$\mathcal{J}_d(\kappa_{mn}^-)\mathcal{Y}_h(\kappa_{mn}^-) - \mathcal{Y}_d(\kappa_{mn}^-)\mathcal{J}_h(\kappa_{mn}^-) = \frac{2\mathrm{i}D_1}{\pi Z_d\beta_{mn}^-}(1-\kappa_{mn}^-M_1)^2\frac{\mathcal{J}_h(\kappa_{mn}^-)}{J_m'(\beta_{mn}^-)}.$$

From Liouville's theorem it follows that the left and right hand sides define the same analytic function. Anticipating smooth enough behaviour at $z=0$ this function is zero, leading to

$$L_+(u)G_+(u) - \mathrm{i}\omega(1-uM_1)F_+(u)\frac{L_+(u)}{\lambda_1}\frac{\mathcal{J}_d(u)\mathcal{Y}_h(u)-\mathcal{Y}_d(u)\mathcal{J}_h(u)}{J_m'(\lambda_1\omega)\mathcal{Y}_h(u)-Y_m'(\lambda_1\omega)\mathcal{J}_h(u)} = \sum_{p=1}^{\infty}\frac{a_{mp}^-}{u-\sigma_{mp}^+} + \sum_{p=1}^{\infty}\frac{c_{mp}^+}{u-\kappa_{mp}^-}, \tag{26d}$$

$$L_-(u)\left\{F_-(u)+\frac{\Psi'_{mn}(1)}{\mathrm{i}\omega(u-\mu^+_{mn})}\right\}-\frac{2\mathrm{i}D_1(1-uM_1)^2L_-(u)}{\pi\omega Z_d\big[\mathcal{J}_d(u)\mathcal{Y}_h(u)-\mathcal{Y}_d(u)\mathcal{J}_h(u)\big]}\left\{\Phi_-(u)-D_1\Psi_{mn}(h)\frac{(1-\mu^+_{mn}M_1)^2}{Z_h(u-\mu^+_{mn})}\right\}=\sum_{p=1}^{\infty}\frac{a^-_{mp}}{u-\sigma^+_{mp}}+\sum_{p=1}^{\infty}\frac{c^+_{mp}}{u-\kappa^-_{mp}}. \tag{26e}$$

Finally we consider equation (24c). Here, the analyticity is violated by the zeros $u=\kappa^+_{mp}$ in the upper half plane, given by

$$J'_m(\beta^+_{mp})\mathcal{Y}_h(\kappa^+_{mp})-Y'_m(\beta^+_{mp})\mathcal{J}_h(\kappa^+_{mp})=0,\ \text{where } \beta^+_{mp}=\lambda_1(\kappa^+_{mp})\omega.$$

Again, we subtract the residue contributions to obtain

$$\begin{aligned}\omega K_+(u)F_+(u)-\sum_{p=1}^{\infty}\frac{c^-_{mp}}{u-\kappa^+_{mp}}&=G_-(u)K_-(u)-D_1\Psi_{mn}(1)\frac{1-\mu^+_{mn}M_1}{u-\mu^+_{mn}}K_-(u)-\sum_{p=1}^{\infty}\frac{c^-_{mp}}{u-\kappa^+_{mp}}\\&-\frac{2\mathrm{i}D_1(1-uM_1)K_-(u)}{\pi\lambda_1\omega\big[J'_m(\lambda_1\omega)\mathcal{Y}_h(u)-Y'_m(\lambda_1\omega)\mathcal{J}_h(u)\big]}\left\{\Phi_-(u)-D_1\Psi_{mn}(h)\frac{(1-\mu^+_{mn}M_1)^2}{Z_h(u-\mu^+_{mn})}\right\}\\&+\mathrm{i}D_1(1-uM_1)\frac{J_m(\lambda_1\omega)\mathcal{Y}_h(u)-Y_m(\lambda_1\omega)\mathcal{J}_h(u)}{\lambda_1\big[J'_m(\lambda_1\omega)\mathcal{Y}_h(u)-Y'_m(\lambda_1\omega)\mathcal{J}_h(u)\big]}\left\{F_-(u)+\frac{\Psi'_{mn}(1)}{\mathrm{i}\omega(u-\mu^+_{mn})}\right\}K_-(u),\end{aligned} \tag{27a}$$

where

$$\begin{aligned}c^-_{mp}=&\frac{2\mathrm{i}D_1(1-\kappa^+_{mp}M_1)K_-(\kappa^+_{mp})}{\pi\beta^+_{mp}\frac{\mathrm{d}}{\mathrm{d}u}\big[J'_m(\lambda_1\omega)\mathcal{Y}_h(u)-Y'_m(\lambda_1\omega)\mathcal{J}_h(u)\big]_{u=\kappa^+_{mp}}}\times\\&\times\left[\frac{\omega\mathcal{J}_h(\kappa^+_{mp})}{\beta^+_{mp}J'_m(\beta^+_{mp})}\left\{F_-(\kappa^+_{mp})+\frac{\Psi'_{mn}(1)}{\mathrm{i}\omega(\kappa^+_{mp}-\mu^+_{mn})}\right\}-\Phi_-(\kappa^+_{mp})+D_1\Psi_{mn}(h)\frac{(1-\mu^+_{mn}M_1)^2}{Z_h(\kappa^+_{mp}-\mu^+_{mn})}\right].\end{aligned} \tag{27b}$$

From Liouville's theorem it follows that the left and right hand sides define the same analytic function. From estimates $K_+\sim u^{3/2}$ in combination with $F_+\sim u^{-1/2}$, without Kutta condition, and $F_+\sim u^{-3/2}$, with Kutta condition, it transpires that this analytic function is in general a constant, say E, which is zero with Kutta condition or maximum vortex shedding. Noting, furthermore, that without vortex shedding no instability is excited, while F_+ does not and K_+ does have a pole in $u=u_0$, we write the constant in the form $E=(1-\Gamma)E_0$, with

$$E_0=-\sum_{p=1}^{\infty}\frac{c^-_{mp}}{u_0-\kappa^+_{mp}},$$

such that $\Gamma=0$ correspond to no vortex shedding and no pole in u_0, while $\Gamma=1$ corresponds to a full Kutta condition. This results in a solution of the form

$$\omega K_+(u)F_+(u)=\sum_{p=1}^{\infty}\frac{c^-_{mp}}{\kappa^+_{mp}-u_0}\left(\frac{u-u_0}{u-\kappa^+_{mp}}-\Gamma\right) \tag{27c}$$

This determines the auxiliary function $F_+(u)$, necessary for the radiated field, and is therefore the main result of this section.

For completeness, we give, from the right-hand side of (27a) also being equal to $(1-\Gamma)E_0$, the relation

$$\begin{aligned}G_-(u)K_-(u)&-\frac{2\mathrm{i}D_1(1-uM_1)K_-(u)}{\pi\lambda_1\omega\big[J'_m(\lambda_1\omega)\mathcal{Y}_h(u)-Y'_m(\lambda_1\omega)\mathcal{J}_h(u)\big]}\left\{\Phi_-(u)-D_1\Psi_{mn}(h)\frac{(1-\mu^+_{mn}M_1)^2}{Z_h(u-\mu^+_{mn})}\right\}\\&+\mathrm{i}D_1(1-uM_1)\frac{J_m(\lambda_1\omega)\mathcal{Y}_h(u)-Y_m(\lambda_1\omega)\mathcal{J}_h(u)}{\lambda_1\big[J'_m(\lambda_1\omega)\mathcal{Y}_h(u)-Y'_m(\lambda_1\omega)\mathcal{J}_h(u)\big]}\left\{F_-(u)+\frac{\Psi'_{mn}(1)}{\mathrm{i}\omega(u-\mu^+_{mn})}\right\}K_-(u)=\\&\sum_{p=1}^{\infty}\frac{c^-_{mp}}{\kappa^+_{mp}-u_0}\left(\frac{u-u_0}{u-\kappa^+_{mp}}-\Gamma\right)+D_1\Psi_{mn}(1)\frac{1-\mu^+_{mn}M_1}{u-\mu^+_{mn}}K_-(u)\end{aligned} \tag{27d}$$

This, however, will not be used here further.

E. Determining the coefficients $a_{mp}^{\pm}$ and $c_{mp}^{\pm}$

As the coefficient a_{mp}^{+} is expressed in the unknown $G_{-}(\sigma_{mp}^{-})$, a_{mp}^{-} in $\Phi_{-}(\sigma_{mp}^{+})$, c_{mp}^{+} in $F_{+}(\kappa_{mp}^{-})$, and c_{mp}^{-} in $F_{-}(\kappa_{mp}^{+})$ and $\Phi_{-}(\kappa_{mp}^{+})$, the solution is not yet known until we have found these coefficients. This, fortunately, is a relatively easy task, since we can set up an infinite system of linear equations by evaluating the pertaining equations at the respective values of u that allows elimination of the unknowns.

From expression (25b) for a_{mr}^{+}, (26d) for $G_{-}(\sigma_{mr}^{-})$, and using the fact that the factor of $F_{+}(\sigma_{mr}^{-})$ vanishes, we obtain for $r = 1, 2, \ldots$

$$a_{mr}^{+}\frac{\pi\omega h Z_h L_{+}(\sigma_{mr}^{-})N_{+}(\sigma_{mr}^{-})}{-2\mathrm{i}D_1(1-\sigma_{mr}^{-}M_1)^2}\frac{\mathrm{d}}{\mathrm{d}u}\big[\mathcal{J}_d(u)\mathcal{Y}_h(u)-\mathcal{Y}_d(u)\mathcal{J}_h(u)\big]_{u=\sigma_{mr}^{-}} = \sum_{p=1}^{\infty}\frac{a_{mp}^{-}}{\sigma_{mr}^{-}-\sigma_{mp}^{+}} + \sum_{p=1}^{\infty}\frac{c_{mp}^{+}}{\sigma_{mr}^{-}-\kappa_{mp}^{-}}. \tag{28a}$$

From expression (26c) for a_{mr}^{-}, (25d) for $\Phi_{-}(\sigma_{mr}^{+})$, we obtain for $r = 1, 2, \ldots$

$$a_{mr}^{-}\frac{\pi\omega Z_d \frac{\mathrm{d}}{\mathrm{d}u}\big[\mathcal{J}_d(u)\mathcal{Y}_h(u)-\mathcal{Y}_d(u)\mathcal{J}_h(u)\big]_{u=\sigma_{mr}^{+}}}{-2\mathrm{i}D_1(1-\sigma_{mr}^{+}M_1)^2 L_{-}(\sigma_{mr}^{+})N_{-}(\sigma_{mr}^{+})} = \sum_{p=1}^{\infty}\frac{a_{mp}^{+}}{\sigma_{mr}^{+}-\sigma_{mp}^{-}} - \frac{D_1\Psi_{mn}(h)(1-\mu_{mn}^{+}M_1)^2}{Z_h N_{-}(\mu_{mn}^{+})(\sigma_{mr}^{+}-\mu_{mn}^{+})}. \tag{28b}$$

From expression (26b) for c_{mr}^{+}, (27c) for $F_{+}(\kappa_{mr}^{-})$, we obtain for $r = 1, 2, \ldots$

$$c_{mr}^{+}\frac{K_{+}(\kappa_{mr}^{-})}{L_{+}(\kappa_{mr}^{-})}\frac{\pi Z_d\beta_{mr}^{-}J_m'(\beta_{mr}^{-})}{2\omega D_1(1-\kappa_{mr}^{-}M_1)^3\mathcal{J}_h(\kappa_{mr}^{-})}\beta_{mr}^{-}\frac{\mathrm{d}}{\mathrm{d}u}[J_m'(\lambda_1\omega)\mathcal{Y}_h(u)-Y_m'(\lambda_1\omega)\mathcal{J}_h(u)]_{u=\kappa_{mr}^{-}} =$$

$$\sum_{p=1}^{\infty}\frac{c_{mp}^{-}}{\kappa_{mp}^{+}-u_0}\left(\frac{\kappa_{mr}^{-}-u_0}{\kappa_{mr}^{-}-\kappa_{mp}^{+}}-\Gamma\right). \tag{28c}$$

From expressions (27b) for c_{mr}^{-}, (26e) for $F_{-}(\kappa_{mr}^{+})$ and $\Phi_{-}(\kappa_{mr}^{+})$, and the definition of κ_{mr}^{+}, we obtain for $r = 1, 2, \ldots$

$$c_{mr}^{-}\frac{L_{-}(\kappa_{mr}^{+})}{K_{-}(\kappa_{mr}^{+})}\frac{\pi\beta_{mr}^{+}J_m'(\beta_{mr}^{+})}{2\mathrm{i}\omega D_1(1-\kappa_{mr}^{+}M_1)\mathcal{J}_h(\kappa_{mr}^{+})}\beta_{mr}^{+}\frac{\mathrm{d}}{\mathrm{d}u}[J_m'(\lambda_1\omega)\mathcal{Y}_h(u)-Y_m'(\lambda_1\omega)\mathcal{J}_h(u)]_{u=\kappa_{mr}^{+}} =$$

$$\sum_{p=1}^{\infty}\frac{a_{mp}^{-}}{\kappa_{mr}^{+}-\sigma_{mp}^{+}} + \sum_{p=1}^{\infty}\frac{c_{mp}^{+}}{\kappa_{mr}^{+}-\kappa_{mp}^{-}}. \tag{28d}$$

The infinite sums in the equations converge very rapidly so they can be truncated quickly.

III. Far Field

From (10b) with (17b) and (17c), the pressure in the ambient mean flow can be expressed as the following integral

$$p_1(r,z) = \frac{\omega^2}{2\pi}\int_L (1-uM_0)^2 F_{+}(u)\frac{H_m^{(2)}(\lambda_0\omega r)}{\lambda_0 H_m^{(2)\prime}(\lambda_0\omega)}\,\mathrm{e}^{-\mathrm{i}\omega u z}\,\mathrm{d}u, \tag{29}$$

where L is the inverse Fourier transform contour.

For the far field ($\omega\sqrt{r^2+z^2} \gg 1$) we can use the asymptotic formula for the Hankel function

$$H_m^{(2)}(\lambda_0\omega r) \sim \sqrt{\frac{2}{\pi\lambda_0\omega r}}\,\mathrm{e}^{-\mathrm{i}(\lambda_0\omega r-\frac{1}{2}m\pi-\frac{1}{4}\pi)}, \tag{30}$$

and replace $H_m^{(2)}(\lambda_0\omega r)$ in (29) to get

$$p_1(r,z) \sim \frac{\omega^2}{2\pi}\int_L (1-uM_0)^2\frac{F_{+}(u)}{\lambda_0 H_m^{(2)\prime}(\lambda_0\omega)}\sqrt{\frac{2}{\pi\lambda_0\omega r}}\,\mathrm{e}^{-\mathrm{i}(\omega\lambda_0 r+\omega u z-\frac{1}{2}m\pi-\frac{1}{4}\pi)}\,\mathrm{d}u. \tag{31}$$

After transforming the free variables

$$r = \varrho\sin\zeta, \qquad z = \varrho\cos\zeta\sqrt{1-M_0^2}, \qquad \omega = \sqrt{1-M_0^2}\,\Omega, \qquad u = \frac{\cos(\zeta-\mathrm{i}\tau)-M_0}{1-M_0^2}, \quad (\tau\in\mathbb{R}), \tag{32}$$

leading to $\lambda_0\omega = \Omega\sin(\zeta - \mathrm{i}\tau)$ and an integration contour L deformed into a branch of a hyperbola $\bar{L}$ (taking account of possible captured pole contributions), we can evaluate the integral by the method of steepest descent (or, which is equivalent here, stationary phase)

$$p_1(r,z) \sim \frac{\mathrm{i}\Omega^2}{2\pi}\,\mathrm{e}^{\mathrm{i}\Omega\varrho M_0\cos\zeta + \mathrm{i}\frac{1}{2}m\pi + \mathrm{i}\frac{1}{4}\pi}\sqrt{\frac{2(1-M_0^2)}{\pi\Omega\varrho\sin\zeta}}\int_{\bar{L}}\frac{(1-uM_0)^2F_+(u)}{H_m^{(2)\prime}(\Omega\sin(\zeta-\mathrm{i}\tau))\sqrt{\sin(\zeta-\mathrm{i}\tau)}}\,\mathrm{e}^{-\mathrm{i}\Omega\varrho\cosh\tau}\,\mathrm{d}\tau, \tag{33}$$

plus in a downtream arc the contribution from the pole in u_0, *i.e.,* the Helmholtz instability. This instability, however, will be further ignored here as in physical reality it will diffuse away. (Note that its acoustic relevance, in the form of its scattering at the trailing edge, is included.) The major contribution to the integral comes from the vicinity of $\tau = 0$,

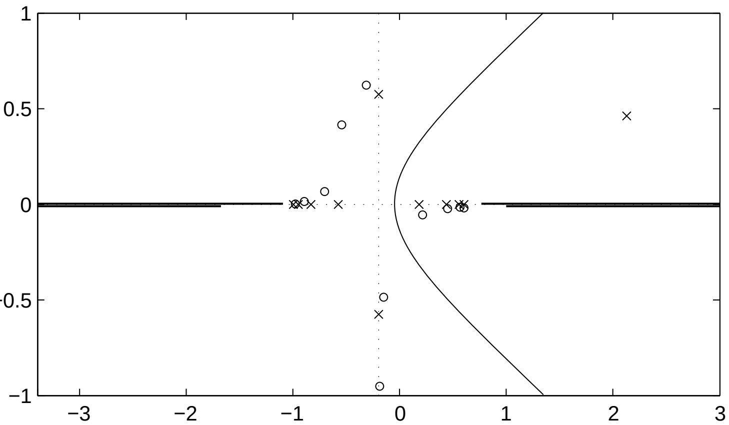

Figure 4. Sketch of steepest descent contour in complex u-plane.

where $\frac{\mathrm{d}}{\mathrm{d}\tau}\cosh\tau = 0$. When we write $\cosh\tau = 1 + \frac{1}{2}\tau^2 + \ldots$, we obtain for large $\Omega\varrho$

$$\int_{-\infty}^{\infty}\mathrm{e}^{-\mathrm{i}\Omega\varrho\cosh\tau}\,\mathrm{d}\tau \simeq \int_{-\infty}^{\infty}\mathrm{e}^{-\mathrm{i}\Omega\varrho-\frac{1}{2}\mathrm{i}\Omega\varrho\tau^2}\,\mathrm{d}\tau = \mathrm{e}^{-\mathrm{i}\Omega\varrho}\int_{-\infty}^{\infty}\mathrm{e}^{-\frac{1}{2}\mathrm{i}\Omega\varrho\tau^2}\,\mathrm{d}\tau = \mathrm{e}^{-\mathrm{i}\Omega\varrho}\,\mathrm{e}^{-\mathrm{i}\frac{1}{4}\pi}\sqrt{\frac{\pi}{\Omega\varrho}}.$$

Hence the solution in the far field can be approximated by

$$p_1(r,z) \sim \frac{\mathrm{i}^{m+1}}{\sqrt{2}\pi}\Omega\frac{(1-M_0\cos\zeta)^2}{(1-M_0^2)^{3/2}}F_+\left(\frac{\cos\zeta - M_0}{1-M_0^2}\right)\frac{\mathrm{e}^{-\mathrm{i}\Omega\varrho(1-M_0\cos\zeta)}}{H_m^{(2)\prime}(\Omega\sin\zeta)\varrho\sin\zeta}. \tag{34}$$

After converting the coordinate variables to the regular physical polar coordinates

$$z = R\cos\varphi, \qquad r = R\sin\varphi, \tag{35}$$

such that

$$\varrho = \frac{R}{\sqrt{1-M_0^2}}\sqrt{1-M_0^2\sin^2\varphi}, \quad \sin\zeta = \frac{\sqrt{1-M_0^2}\sin\varphi}{\sqrt{1-M_0^2\sin^2\varphi}}, \quad \cos\zeta = \frac{\cos\varphi}{\sqrt{1-M_0^2\sin^2\varphi}},$$

we obtain

$$p_1(R,\varphi) \sim \frac{D_p(\varphi)}{R}\exp\left(-\mathrm{i}\frac{\omega}{1-M_0^2}R\left(\sqrt{1-M_0^2\sin^2\varphi} - M_0\cos\varphi\right)\right) \tag{36}$$

where pressure field directivity D_p is given by

$$D_p(\varphi) = \frac{\mathrm{i}^{m+1}}{\sqrt{2}\pi}\frac{\omega}{(1-M_0^2)^2}\frac{(1-M_0\cos\zeta)^2}{H_m^{(2)\prime}(\Omega\sin\zeta)\sin\varphi}F_+\left(\frac{\cos\zeta - M_0}{1-M_0^2}\right) \tag{37}$$

What remains is the numerical calculation of F_+ of (27c).

IV. Numerical evaluation

Since $\log(N(u)), \log(L(u)), \log(K(u)) \sim \pm\log|u|$ for $|u| \to \infty$, the integrals (23) for the split functions do not converge normally at infinity, and we have to convert it into a Cauchy Principle Value integral [18, p.42]. We take the limit symmetrically around a suitable real number between the branch points of λ_0 and λ_1 that separates the right and left running modes (this is not always possible, in which case the contribution of the missed poles have to be added as residues; see [7,8]). Without going into every detail, we obtain typically a contour as depicted in figure 5. More details can be found in [19,20]. An important point to be checked is whether anywhere along the contour $K(u)$ crosses the branch cut of the logarithm function, normally chosen along the negative real axis. In such a case the integrand is not analytic and the split integral is invalid.

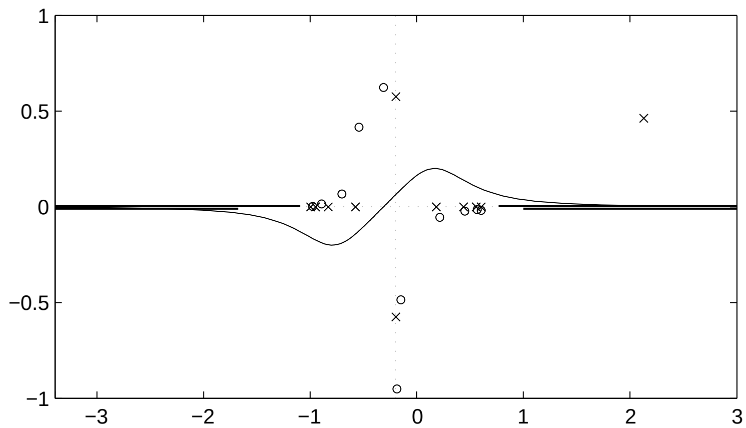

Figure 5. Sketch of deformed integration contour for splitfunctions in u-plane.

V. Numerical Examples

A series of examples are numerically evaluated to see the effect of the lined afterbody, with and without jet flow and duct lining. The problem parameters are chosen from the data set of the experiments of De Mercato, Tester and Holland [2].

For zero flow, the outer and jet properties are the same, where outer flow values are used in both regions. The far field values are plotted dimensionally, at a distance 46.0 m away from the exhaust plane. The incident mode amplitude is taken such that the cross-sectional averaged intensity at $z = 0$ is 1 W/m^2.

The geometry parameters that were used are

R_h		$= 0.1191$ m	M_j	$= U_j/c_j$	$= 0.5$	ρ_0		$= 1.225$ kg/m^3
R_d		$= 0.1985$ m	ρ_j		$= 1.1921$ kg/m^3	M_1	$= U_j/c_0$	$= 0.507026$
h	$= R_h/R_d$	$= 0.6$	U_0		$= 0$ m/s	C_1	$= c_0/c_j$	$= 0.986143$
U_j		$= 172.475$ m/s	c_0		$= 340.17$ m/s	D_1	$= \rho_j/\rho_0$	$= 0.973143$
c_j		$= 344.95$ m/s	M_0	$= U_0/c_0$	$= 0$			

all with full Kutta condition, in combination with the following frequencies and impedances

f_1		$= 1250$ Hz	Z_d	(duct)	$= 1 - 7.27$i			
ω_1	$= 2\pi f_1 R_d/c_0$	$= 4.58305$	Z_h	(afterbody)	$= 1 - 7.27$i			
m		$= 0$	μ_{01}^+	(hard)	$= 0.6574286$	μ_{01}^+	(soft)	$= 0.67753 - 0.00275$i
m		$= 1$	μ_{11}^+	(hard)	$= 0.6183997$	μ_{11}^+	(soft)	$= 0.64072 - 0.00305$i

f_5		$= 3150$ Hz	Z_d	(duct)	$= 1 - 2.79\mathrm{i}$			
ω_1	$= 2\pi f_5 R_d/c_0$	$= 11.54928$	Z_h	(afterbody)	$= 1 - 2.79\mathrm{i}$			
m		$= 0$	μ_{01}^+	(hard)	$= 0.6574286$	μ_{01}^+	(soft)	$= 0.67923 - 0.00925\mathrm{i}$
m		$= 5$	μ_{51}^+	(hard)	$= 0.5043326$	μ_{51}^+	(soft)	$= 0.54708 - 0.01718\mathrm{i}$

f_6		$= 4000$ Hz	Z_d	(duct)	$= 1 - 2.14\mathrm{i}$			
ω_1	$= 2\pi f_6 R_d/c_0$	$= 14.66575$	Z_h	(afterbody)	$= 1 - 2.14\mathrm{i}$			
m		$= 6$	μ_{61}^+	(hard)	$= 0.5243871$	μ_{61}^+	(soft)	$= 0.56989 - 0.02547\mathrm{i}$
			μ_{62}^+	(hard)	$= 0.3054997$	μ_{62}^+	(soft)	$= 0.34767 - 0.01544\mathrm{i}$

In the following sets of cases the effect of adding a lined afterbody to a hard-walled duct and a lined duct, with and without flow is considered. Note that it is not possible to compare the radiation of the hard-walled duct with the lined duct, because the location of the source, and hence the attained damping, is unknown. Therefore, we will only compare the adding of the afterbody liner with a reference situation of a hard-walled duct and with another reference situation of the lined duct.

A. Frequency f_1

The 1st set, given in figure 6, shows the field of the first radial $m = 0$-mode for a relatively low frequency and a relatively high impedance. The 2nd set, given in figure 7, shows the corresponding first radial $m = 1$-mode. Adding the afterbody liner gives only a slight reduction in all cases. This is probably due to the high impedance used.

B. Frequency f_5

The 3d set, given in figure 8, shows the field of the first radial $m = 0$-mode for a higher frequency and a moderate impedance. The 4th set, given in figure 9, shows the corresponding first radial $m = 5$-mode. Adding the afterbody liner gives a considerable reduction in the downstream arc without flow, which broadly agrees with the findings of [2]. With flow this reduction is much less.

C. Frequency f_6

The 5th and 6th sets, given in figures 10 and 11, show the fields of the first and second radial $m = 6$-modes for a rather higher frequency and a moderate impedance. Again, adding the afterbody liner gives by and large a reasonable reduction in the downstream arc without flow, while with flow this reduction is much less, and only in the upstream arc.

VI. Conclusions

Experimental evidence for the no-flow configuration by Tester et al. [1,2] showed that a lined afterbody could have an overall beneficial effect on the radiation field from an exhaust duct by as much as 1 to 4 dB. The presence of mean flow however, addressed by numerical simulation in [3], seemed to limit this reduction.

In order to produce a complementary, fully exact, solution of Wiener-Hopf type that could (in principle) compare these cases, we developed the present model of sound radiation from a semi-infinite duct, with jet flow and co-flow while the duct is lined on the inside of the outer wall, and a doubly infinite hub that is lined on the part outside the duct.

The Wiener-Hopf solution for this kind of problems is non-standard and quite formidable, because the usual factorisation is not possible, and we have to resort to the so-called weak factorisation method.

The formal solution has been implemented numerically, and the results obtained showed (for the limited number of cases considered) by and large a confirmation of the conclusions of Tester et al. More extended parameter scans for more impedance values should be done to see if impedances are possible that retain with flow the interesting attenuations achieved without flow.

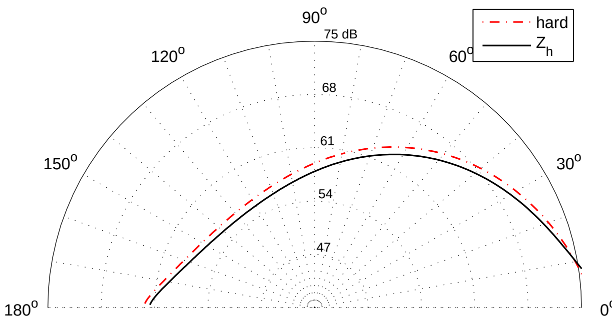

(a) No flow, hard duct

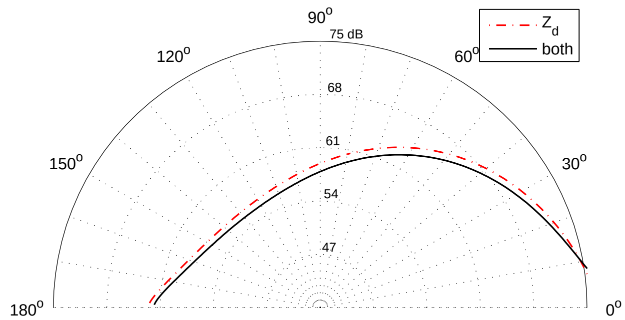

(b) No flow, lined duct

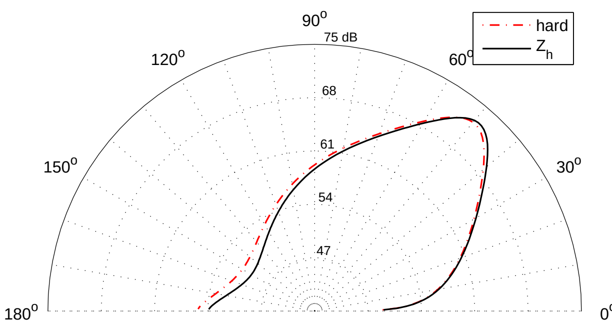

(c) With flow, hard duct

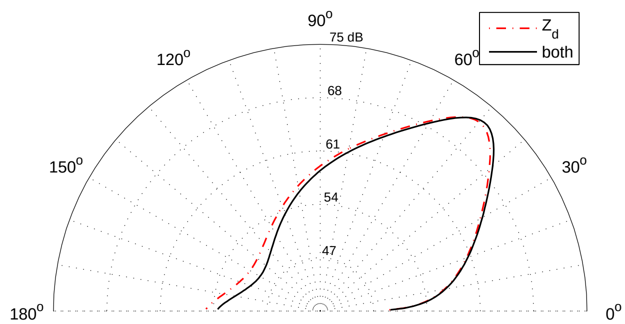

(d) With flow, lined duct

Figure 6. Frequency f_1 with $m = 0$ and the 1st radial mode

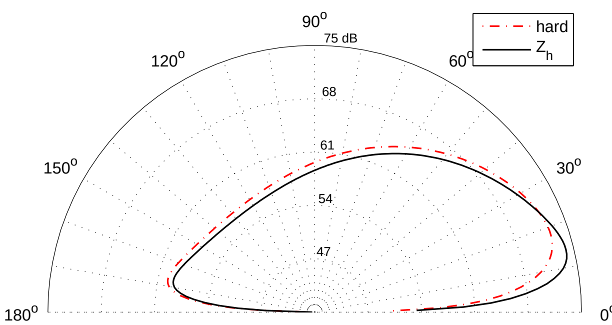

(a) No flow, hard duct

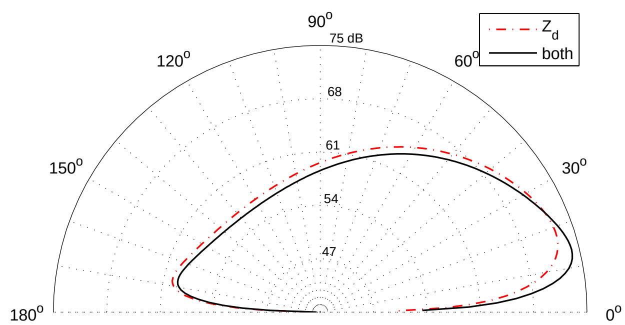

(b) No flow, lined duct

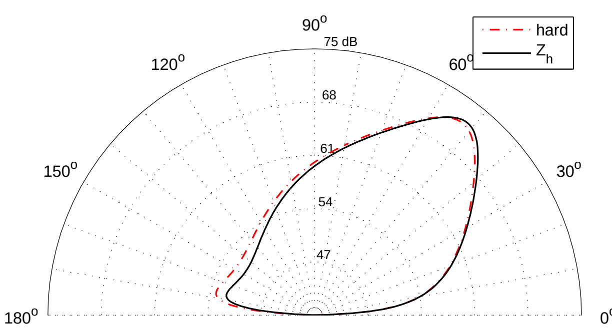

(c) With flow, hard duct

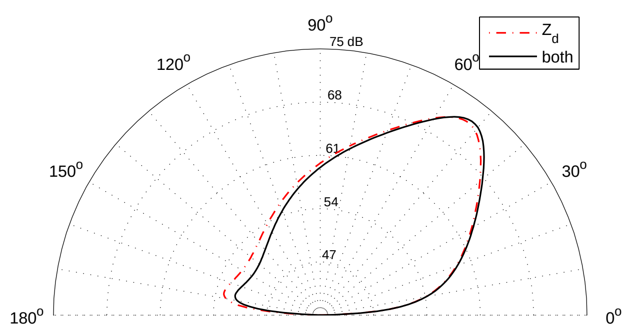

(d) With flow, lined duct

Figure 7. Frequency f_1 with $m = 1$ and the 1st radial mode

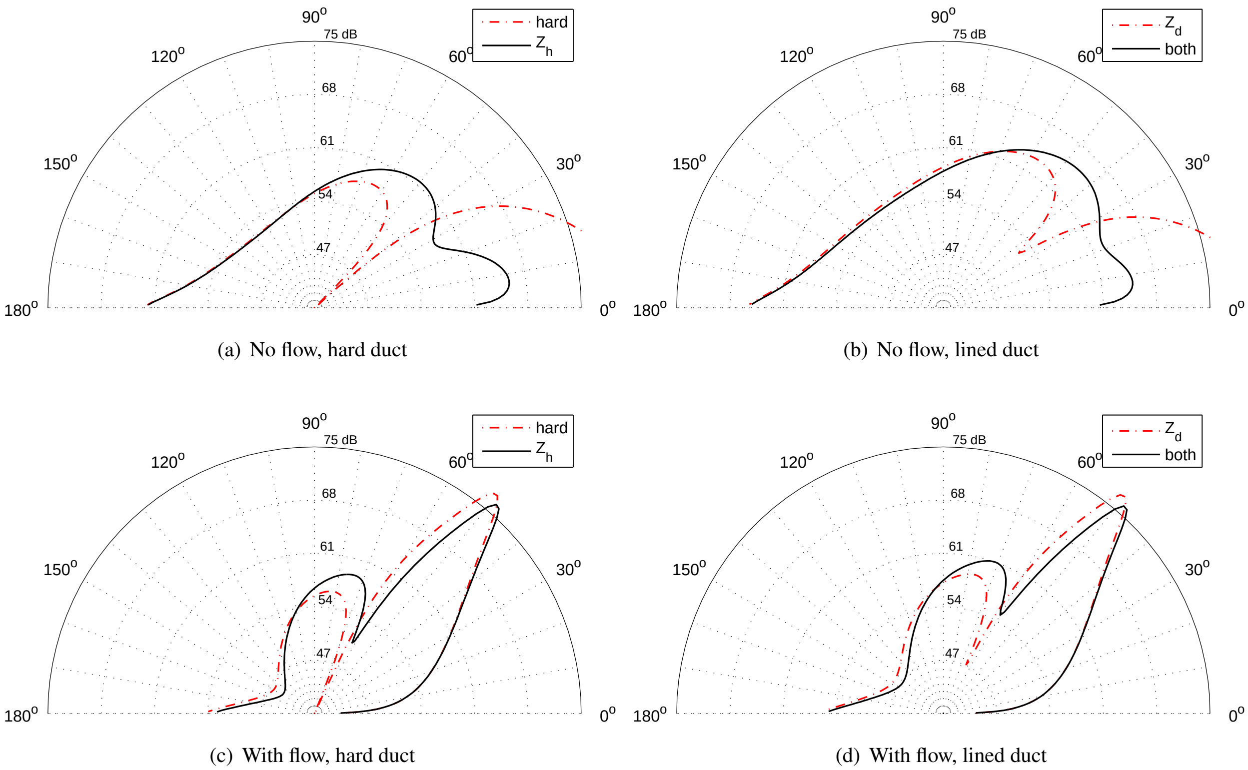

(a) No flow, hard duct (b) No flow, lined duct

(c) With flow, hard duct (d) With flow, lined duct

Figure 8. Frequency f_5 with $m = 0$ and the 1st radial mode

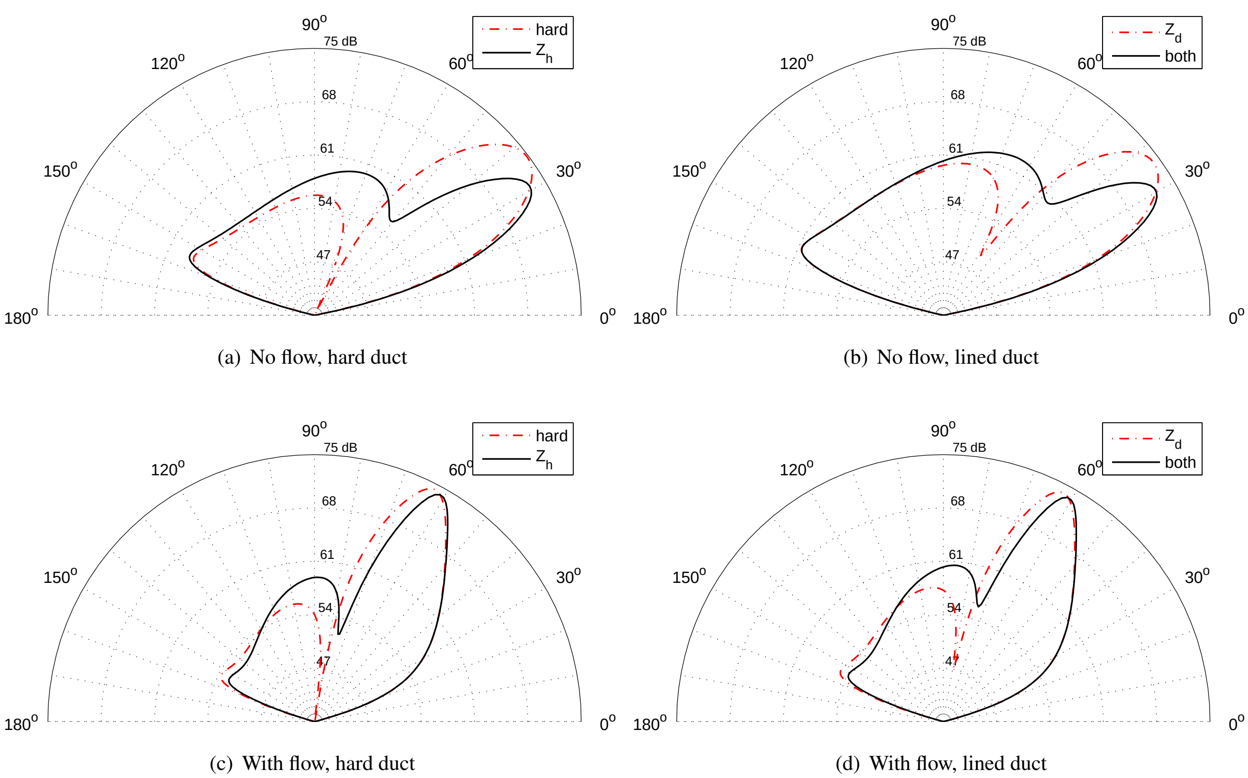

(a) No flow, hard duct (b) No flow, lined duct

(c) With flow, hard duct (d) With flow, lined duct

Figure 9. Frequency f_5 with $m = 5$ and the 1st radial mode

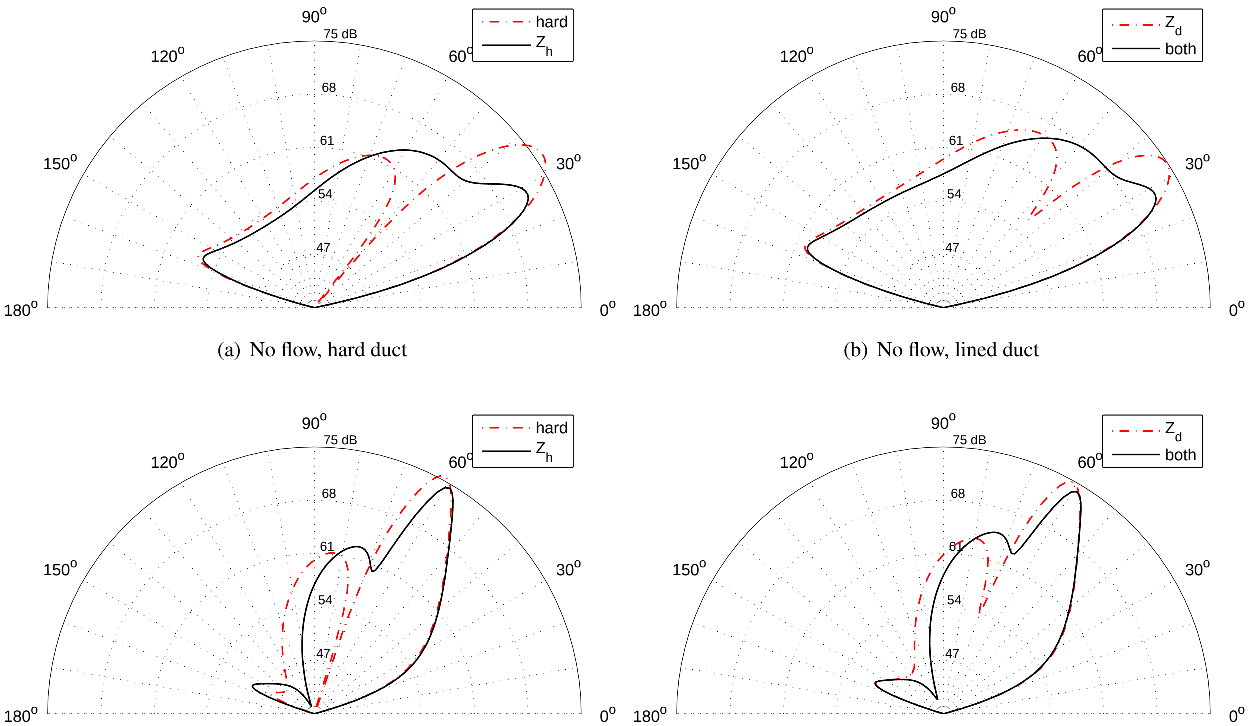

(a) No flow, hard duct

(b) No flow, lined duct

(c) With flow, hard duct

(d) With flow, lined duct

Figure 10. Frequency f_6 with $m = 6$ and the 1st radial mode

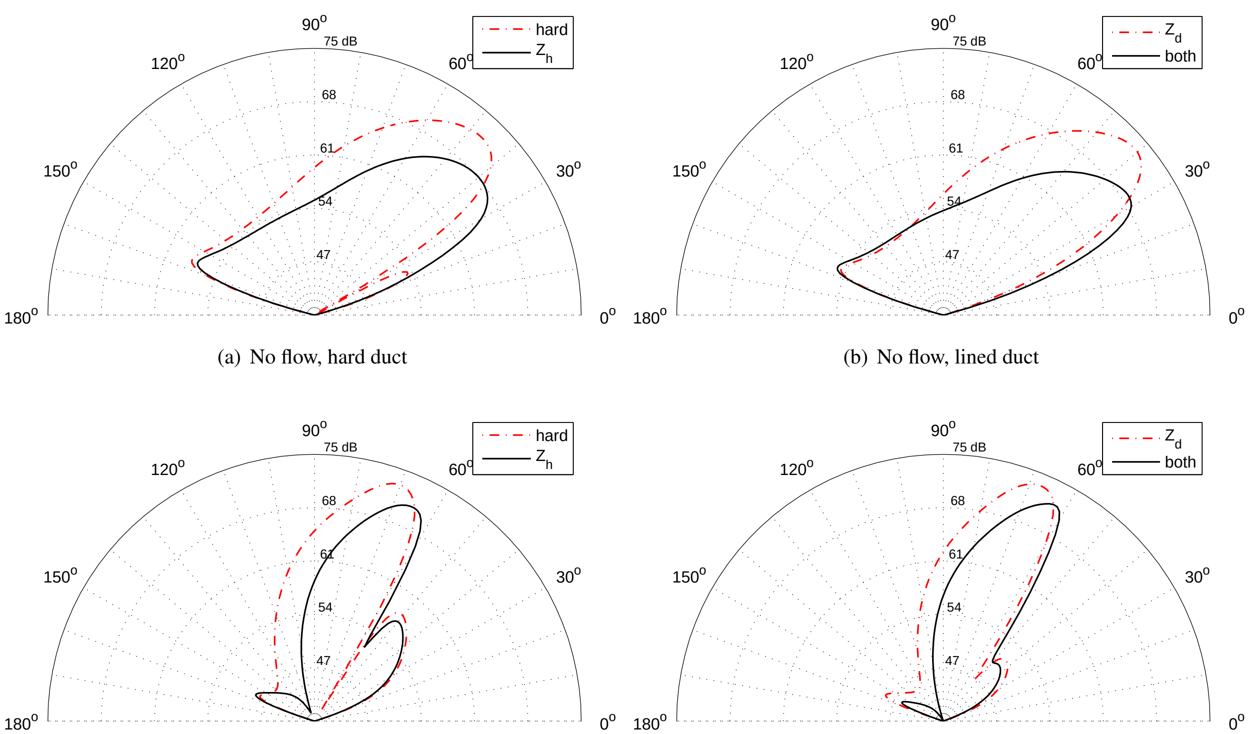

(a) No flow, hard duct

(b) No flow, lined duct

(c) With flow, hard duct

(d) With flow, lined duct

Figure 11. Frequency f_6 with $m = 6$ and the 2nd radial mode

VII. Acknowledgement

The present work was inspired by, and a continuation of, our work carried out under the European collaborative project "TURNEX" under the Sixth Framework Programme (Technical Officer Daniel Chiron, Project Coordinator Brian Tester). We would like to express our appreciation for the cooperation with the partners of the project.

References

[1] B.J. Tester, L. De Mercato and K. Holland, Aft fan noise reduction with a lined afterbody. AIAA 2007-3527 of the 13th AIAA/CEAS Aeroacoustics Conference, 2007

[2] L. De Mercato, B.J. Tester and K. Holland, Aft fan noise reduction with a lined afterbody. Paper 431 of the 14th ICSV, Cairns, Australia, 2007

[3] L. De Mercato and B.J. Tester, After-body Liner Performance Predictions. AIAA 2008-2881 of the 14th AIAA/CEAS Aeroacoustics Conference, 2008

[4] A. Demir and S.W. Rienstra, Sound Radiation from an Annular Duct with Jet Flow and a Lined Centerbody, AIAA 2006-2718 of the 12th AIAA/CEAS Aeroacoustics Conference, Cambridge, MA, 8-10 May 2006

[5] R.M. Munt. The interaction of sound with a subsonic jet issuing from a semi-infinite cylindrical pipe. *Journal of Fluid Mechanics*, 83(4):609-640, 1977.

[6] S.W. Rienstra, Acoustic Radiation From A Semi-Infinite Annular Duct In A Uniform Subsonic Mean Flow, *Journal of Sound Vibration*, 94(2):267-288, 1984

[7] G. Gabard, R. Astley and M. Ben Tahar Noise Radiation from a Jet Pipe: A Benchmark Problem for Computational Aeroacoustics AIAA-2005-3064 11th AIAA/CEAS Aeroacoustics Conference, 23-25 May 2005

[8] G. Gabard and R.J. Astley, Theoretical models for sound radiation from annular jet pipes: far- and near-field solutions, *Journal of Fluid Mechanics*, 549:315-342, 2006

[9] H. Levine and J. Schwinger. On the radiation of sound from an unflanged circular pipe. *Physical Review*, 73:383-406, 1948

[10] G.F. Carrier. Sound transmission from a tube with flow. *Quarterly of Applied Mathematics*, 13:457-461, 1956.

[11] A. Demir and S.W. Rienstra, Sound Radiation from a Buried Nozzle with Jet and Bypass Flow, paper no. 449 at ICSV14, the Fourteenth International Congress on Sound and Vibration, Cairns, July 9-12, 2007.

[12] B. Veitch and N. Peake, Acoustic propagation and scattering in the exhaust flow from coaxial cylinders, *Journal of Fluid Mechanics*, 613, 275-307, 2008

[13] M. Idemen, A new method to obtain exact solutions of vector Wiener-Hopf equations, ZAMM 59:656-658, 1979

[14] A. Büyükaksoy and A. Demir, Radiation of sound from a semi-infinite rigid duct inserted axially into a larger infinite tube with wall impedance discontinuity, ZAMM (in press)

[15] I.D. Abrahams, Scattering of sound by two parallel semi-infinite screens, Wave Motion 9:289-300, 1987

[16] K.U. Ingard, Influence of Fluid Motion Past a Plane Boundary on Sound Reflection, Absorption, and Transmission, *Journal of the Acoustical Society of America* 31(7), 1035–1036, 1959

[17] M.K. Myers, On the acoustic boundary condition in the presence of flow, *Journal of Sound and Vibration*, 71 (3), p.429–434, 1980

[18] B. Noble, *Methods based on the Wiener-Hopf Technique*, Pergamon Press, London, 1958.

[19] S.W. Rienstra and N. Peake, Modal Scattering at an Impedance Transition in a Lined Flow Duct, AIAA 2005-2852 of the 11th AIAA/CEAS Aeroacoustics Conference, Monterey, CA, 23-25 May 2005

[20] S.W. Rienstra, Acoustic Scattering at a Hard-Soft Lining Transition in a Flow Duct, Journal of Engineering Mathematics, 59(4), 2007